

**AWARD NUMBER:**  
W81XWH-18-C-0047

**TITLE:**  
Biofidelic Rat Testing Device (RTD) to Measure Blast Exposure and Loadings for TBI

**PRINCIPAL INVESTIGATOR:**  
Mr. Keith Sedberry

**CONTRACTING ORGANIZATION:**  
CFD Research Corporation  
Huntsville, AL 35806

**REPORT DATE:** July 2018

**TYPE OF REPORT:**  
Phase 1 Final

**PREPARED FOR:** U.S. Army Medical Research and Materiel Command  
Fort Detrick, Maryland 21702-5012

**DISTRIBUTION STATEMENT:** Approved for Public Release;  
Distribution Unlimited (STTR Data Rights)

The views, opinions and/or findings contained in this report are those of the author(s) and should not be construed as an official Department of the Army position, policy or decision unless so designated by other documentation.

# REPORT DOCUMENTATION PAGE

*Form Approved*  
*OMB No. 0704-0188*

Public reporting burden for this collection of information is estimated to average 1 hour per response, including the time for reviewing instructions, searching existing data sources, gathering and maintaining the data needed, and completing and reviewing this collection of information. Send comments regarding this burden estimate or any other aspect of this collection of information, including suggestions for reducing this burden to Department of Defense, Washington Headquarters Services, Directorate for Information Operations and Reports (0704-0188), 1215 Jefferson Davis Highway, Suite 1204, Arlington, VA 22202-4302. Respondents should be aware that notwithstanding any other provision of law, no person shall be subject to any penalty for failing to comply with a collection of information if it does not display a currently valid OMB control number. **PLEASE DO NOT RETURN YOUR FORM TO THE ABOVE ADDRESS.**

<b>1. REPORT DATE (DD-MM-YYYY)</b> July 2018		<b>2. REPORT TYPE</b> Final, Phase I		<b>3. DATES COVERED (From - To)</b> 11 Dec 2017 - 10 Jun 2018	
<b>4. TITLE AND SUBTITLE</b> Biofidelic Rat Testing Device (RTD) to Measure Blast Exposure and Loadings for TBI				<b>5a. CONTRACT NUMBER</b> W81XWH-18-C-0047	
				<b>5b. GRANT NUMBER</b>	
				<b>5c. PROGRAM ELEMENT NUMBER</b>	
<b>6. AUTHOR(S)</b> Keith Sedberry, Vincent Harrant, Andrzej Przekwas – CFDRRC Maciej Skotak, Molly Townsend, Namas Chandra - NJIT				<b>5d. PROJECT NUMBER</b>	
				<b>5e. TASK NUMBER</b>	
				<b>5f. WORK UNIT NUMBER</b>	
<b>7. PERFORMING ORGANIZATION NAME(S) AND ADDRESS(ES)</b> CFD Research Corporation 701 McMillian Way NW Suite D Huntsville, AL 35806				<b>8. PERFORMING ORGANIZATION REPORT NUMBER</b>  9312/Final	
<b>9. SPONSORING / MONITORING AGENCY NAME(S) AND ADDRESS(ES)</b>  U.S. Army Medical Research and Materiel Command Fort Detrick, Maryland 21702-5012				<b>10. SPONSOR/MONITOR'S ACRONYM(S)</b>	
				<b>11. SPONSOR/MONITOR'S REPORT NUMBER(S)</b>	
<b>12. DISTRIBUTION / AVAILABILITY STATEMENT</b>  Approved for Public Release; Distribution Unlimited					
<b>13. SUPPLEMENTARY NOTES</b> STTR DATA Rights					
<b>14. ABSTRACT</b> The overall objective of this project (Phase I, II, and III) is to develop, fabricate, and test a novel biofidelic rat surrogate for the validation of primary blast loading conditions for mild traumatic brain injury (mTBI). The Phase I work summarized in this Final Report shows the CFDRRC/NJIT team was able to create a state of the art and first of it's kind rat test device (RTD) to measure blast loadings in experimental inside a shock tube meant to mimic field blast conditions in a repeatable manner. A complementary virtual shock tube was also created to allow for predictive investigations of loading scenarios on the RTD to help guide future investigations and experiments and was partially validate for 3-D. This approach, a coupled experimental and computational investigation tool, will prove value to the Army to study blast loadings without live animals and also give a common/singular test bed for future TBI research relating to rat/human blast loadings. The desire of the CFDRRC/NJIT team is to expand the RTD to include other test article options to create a suite of Blast Test Devices to assist in future blast investigations to the community at large. There remains no good way to correlate individual blast studies and investigations as each study uses different set-ups and devices with no common link. A suite of blast test devices could go a long way in linking these studies together and take a firm step towards creating defined blast standards for PPE and warfighter exposure.					
<b>15. SUBJECT TERMS</b> Traumatic Brain Injury (TBI), Blast Loading, Rat Surrogate, Shock Tube, Injury, Biofidelic					
<b>16. SECURITY CLASSIFICATION OF:</b> SAR			<b>17. LIMITATION OF ABSTRACT</b>	<b>18. NUMBER OF PAGES</b>	<b>19a. NAME OF RESPONSIBLE PERSON</b> USAMRMC
<b>a. REPORT</b> U	<b>b. ABSTRACT</b> U	<b>c. THIS PAGE</b> U			<b>19b. TELEPHONE NUMBER (include area code)</b>
			UU	42	

## TABLE OF CONTENTS

	<b>Page No.</b>
1. INTRODUCTION: .....	1
2. OVERALL PROJECT SUMMARY: .....	2
3. KEY RESEARCH ACCOMPLISHMENTS: .....	29
4. CONCLUSION:.....	30
5. PUBLICATIONS, ABSTRACTS, AND PRESENTATIONS:.....	31
6. INVENTIONS, PATENTS AND LICENSES: .....	32
7. REPORTABLE OUTCOMES:.....	33
8. OTHER ACHIEVEMENTS:.....	34
9. REFERENCES: .....	35
10. APPENDICES: .....	36

## LIST OF FIGURES

	<b>Page No.</b>
Figure 1. 3D surface STL of a rat head (left) and physical 3D printed rat skin, skull, and brain (right) .....	3
Figure 2. Simplified Rat Head .....	4
Figure 3. Before and after outliers were removed from measured and expected data.....	5
Figure 4. 50 <sup>th</sup> Percentile Rat Body 2D drawing with measurements.....	6
Figure 5. Anatomical rat geometry .....	7
Figure 6. Non-descript rat geometry.....	7
Figure 7. RTD geometry (colored in teal) overlaid on anatomical rat geometry (colored in blue).....	8
Figure 8. NJIT 9” Shock Tube schematic .....	8
Figure 9. Experimental shock tube pressure traces for 10 psi target exposure (at various locations).....	9
Figure 10. Experimental shock tube pressure traces for 10 psi target exposure (at T4 location) .....	10
Figure 11. Virtual schematic of the NJIT 9” shock tube with pressure sensor location offsets ..	10
Figure 12. 3-D model of NJIT 9” shock tube in CFD-GEOM before meshing.....	11
Figure 13. Structured mesh in CFD-GEOM representing the 9” NJIT shock tube .....	11
Figure 14. 1D to 3D mesh linking .....	13
Figure 15. Example of flow pressure (top) and velocity vectors colored by pressure (bottom) in 1D to 3D mixed grid. ....	14
Figure 16. 10 psi NJIT shock tube data at T4 sensor.....	15
Figure 17. Experimental & 1D CoBi wire model comparison .....	15
Figure 18. Exterior overview of the assembled RTD prototype.....	17
Figure 19. Interior overview of the RTD prototype showing sensor mounting and wiring .....	17
Figure 20. The shock tube testing of the latest version of the RTD. Details of the sensor location and wiring (A, B), the assembled model (C), and the instrumented model mounted in the shock tube (D).....	19
Figure 21. Experimental Shock Tube testing set-up with new micro ICP sensors in RTD.....	20
Figure 22. The test experiment at nominal shock wave intensity of 10 psi (134A sensor). Micro ICP sensors were connected by-passing signal conditioner using the polarity from product manual (black lead (+), silver lead (-)). .....	20
Figure 23. The test experiment at nominal shock wave intensity of 10 psi (134A sensor). Micro ICP sensors were connected by-passing signal conditioner using the polarity from product manual (black lead (+), silver lead (-)). .....	21
Figure 24. The test experiment at nominal shock wave intensity of 10 psi (134A sensor). Micro ICP sensors were connected via signal conditioner using reversed polarity (black lead (-), silver lead (+))......	21
Figure 25. The test experiment at nominal shock wave intensity of 10 psi (134A sensor). Micro ICP sensors were connected via signal conditioner using reversed polarity (black lead (-), silver lead (+))......	22
Figure 26. The test experiment at nominal shock wave intensity of 5 psi (134A sensor). Micro ICP sensors were connected via signal conditioner using reversed polarity (black lead (-), silver lead (+))......	22

Figure 27. The test experiment at nominal shock wave intensity of 5 psi (134A sensor). Micro ICP sensors were connected via signal conditioner using reversed polarity (black lead (-), silver lead (+))...... 23

Figure 28. The 3<sup>rd</sup> generation 3D printed RTD prototype instrumented with three pressure sensors during the shock tube testing. The prototype is mounted in the inside (A, B) and outside locations (C, D). ..... 24

Figure 29. The RTD testing in the shock tube: inside location. The representative pressure profiles recorded by the incident pressure sensor (T4) mounted in the shock tube wall, and three pressure sensors mounted in the RTD prototype and exposed to a single shock wave with nominal intensity of: A) 70 kPa, B) 130 kPa, and C) 180 kPa. The quantification of the peak overpressure values is presented in figure D. Tests were repeated four times at each nominal shock wave intensity. .... 25

Figure 30. The RTD testing in the shock tube: outside location. The representative pressure profiles recorded by the incident pressure sensor (T4) mounted in the shock tube wall, and three pressure sensors mounted in the RTD prototype and exposed to a single shock wave with nominal intensity of: A) 70 kPa, B) 130 kPa, and C) 180 kPa. The quantification of the peak overpressure values is presented in figure D. Tests were repeated four times at each nominal shock wave intensity. .... 26

Figure 31. Test specimen area in 3D simulation environment ..... 27

Figure 32. Experimental results compared to 1D and 3D simulation results ..... 27

## LIST OF TABLES

	<b>Page No.</b>
Table 1. Length between each landmark on rat head.....	3
Table 2. Heights and Widths of each Landmark.....	4
Table 3. 50 <sup>th</sup> Percentile Rat Body Measurements.....	5
Table 4. Experimental Shock Tube Parameters for 10 psi test .....	9

## **1. INTRODUCTION:**

In the last few years the US Department of Defense (DoD) has initiated a significant research program to understand the mechanisms of blast brain injury and protection [Leggieri 2009]. Return from these efforts was overall rather insignificant considering at the time the program was initiated there were no standardized criteria for blast TBI animal models, and a number of independently developed models in different laboratories suffered from major shortcomings: 1) animals were frequently tested outside of the shock tube, which doesn't represent field conditions, and 2) often animal head was not restrained which resulted in acceleration-deceleration type of TBI instead of primary blast. Thus, considering there is an urgent demand to accelerate the fielding of prevention and treatment strategies by leveraging existing knowledge and fostering collaboration and information sharing by the blast injury research community [Gupta, 2013]. Live animal testing and full scale experimental cadaver blast testing, which are two environments to study TBI causing exposures, can be expensive and time consuming. Further, with respect to animal models and specifically rats, there is an overwhelming amount of research that varies across many parameters including specimen choice, shock tube/blast exposure levels, and other biochemical/biomedical observations. The overall objective of this project (Phase I, II, and III) is to develop, fabricate, and test a novel biofidelic rat surrogate for the validation of primary blast loading conditions. In long term perspective this device will be used to standardize exposure conditions in bTBI research area and will allow comparison of experimental data between laboratories, and more effective distribution of funding addressing various aspects of bTBI etiology and diagnostics.

## 2. OVERALL PROJECT SUMMARY:

The goal of Phase I was to develop a rat surrogate geometry, instrumentation layout, material selection, and preliminary testing with computational validation for blast loadings for mild TBI investigations. To achieve this goal, the specific objectives for the Phase I are summarized as follows:

- Analyze existing rat biometric databases at CFDRC/NJIT and complete a statistical analysis on the populations. The focus here will be on Sprague Dawley (SD) rats as they represent dominant species used in the bTBI research area, our team has extensive experience in blast testing and large amount of data on this specific animal model. A 50<sup>th</sup> percentile geometry will be derived from this database population analysis.
- Using the data from the statistical analysis on the rat databases, a high resolution computational model will be generated. This model will be used in computational blast environments and compared to a lower resolution model that will be used for physical rat surrogate production. Instrumentation sites and configurations will also be explored in this computational framework for potential issues and sensitivities.
- The results of the simulations will be used to formulate specific design specifications for the physical rat surrogate prototype. A down select of materials and instrumentation for the rat surrogate will also be conducted.
- Next, a physical rat prototype will be produced in a rigid and semi-flexible format for comparison and evaluation of the material selection. These preliminary prototypes will be provided to the Army for feedback at the end of the Base program.
- The preliminary prototype will be tested in a shock tube environment under field-validated blast loading conditions in the prone position at various pressure magnitudes. High speed video will also be used to capture the motion of the rat prototype for evaluation and comparison. The results of these experimental tests will be compared to the earlier simulations for numerical validated of the rat testing device (RTD).
- Finally, available data and designs captured during the Phase I effort will be packaged and delivered to the Army along with a detailed report. Trade-offs and correlations between pool of possible solution(s) and the existing models will be provided. Recommendations and a Preliminary Design for the complete rat testing device solution will be given to the Army on the methodology (fabrication, experimental testing and validation protocols) that will be used to create the RTD solution(s) in the Phase II effort. Specific plans for the Phase II effort, including how to produce the RTD, the optimization plan for the RTD, and the complementary computational investigation protocols will be presented during a visit to the Army at the end of the Phase I effort.

The CFDRC/NJIT team is pleased to report that all goals were met during the Phase I effort.

### Task 1. Creation of 50<sup>th</sup> Percentile Rat Geometry and Virtual Model

The first step in the creation of the 50<sup>th</sup> percentile RTD was to focus on the head. This area is especially important in blast loadings so considerations were made into shape, prototype, manufacturability, and to ensure that the head could be instrumented with an array of sensors. Another important aspect of the head is the geometric shape as different angles will influence how

a pressure wave is loaded onto those angles. These loadings could be artificially enhanced or lowered on the RTD if the shape isn't representative of the real rat geometry.

One important consideration when creating the RTD geometry was the decision to include an outer layer of fur. While fur should be considered in part of the mass and shape of the rat, past work has shown that fur can cause issues with instrumentation and video of the rat during a blast loading. Producing a synthetic fur on any RTD would require meticulous work and drive both the time required to create an RTD and the cost. Repeatability of a RTD with fur would also be difficult if the synthetic fur was not stable and secured to the skin. Taking all these factors into account, fur was not included in the RTD produced in this program. However, the fur's mass and shape were taken into account when the RTD geometry design was evaluated.

The center for injury biomechanics, materials and methods (CIBM<sup>3</sup>) used MRI and CT scans on rats to obtain rat image data. The images were separated into outer skin, skeleton, and brain for separate 3D models. Using commercial software, the images were converted in 3D solids as described in the book "Brain Neurotrauma: Molecular, Neuropsychological and Rehabilitation Aspects" (Chandra and Sundaramurthy). 3D printed versions of the skin, skull, and brain were created to assist in the physical measurements of the rats. Figure 1 shows the 3D surface of the outer layer of the skin from the original MRI scan in an STL format as well as the 3D printed rat skin, skull, and brain.

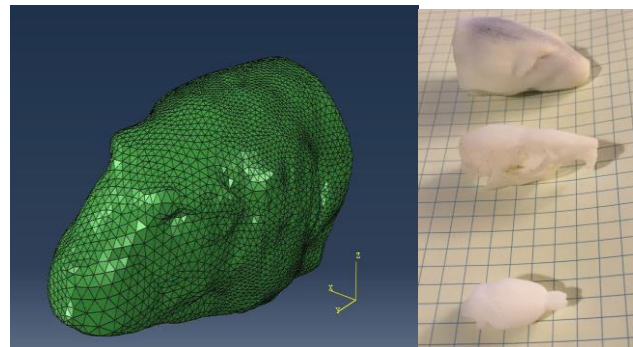


Figure 1. 3D surface STL of a rat head (left) and physical 3D printed rat skin, skull, and brain (right)

Measurements were taken of the 3D printed structures to get a rough estimate of the geometry of the rat head. Landmarks were chosen on the rat head for these measurements. They included the tip of the nose, the stop (proximal end of the rat's muzzle), the brow, peak of the head, crown, and the edge of the skull. Measurements were obtained at lengths between these points and the data is presented in Table 1 below.

**Table 1. Length between each landmark on rat head**

Points	Locations	Length between (mm)
1-2	Nose to stop	14.3
2-3	Stop to brow	10.2
3-4	Brow to peak	7.3
4-5	Peak to crown	10.3
5-6	Crown to edge	2.7

To assist in simplifying the geometry of the head for future RTD prototype production, the height and width of each measured area was recorded. This allowed for elliptical shapes to be created for

each area which will make up the computational and physical RTD. The measurements of those areas are shown below in Table 2.

**Table 2. Heights and Widths of each Landmark**

Point	Location	Height (mm)	Width (mm)
1	Nose	7.51	7.51
2	Stop	18.15	18.15
3	Brow	24.00	28.00
4	Peak	29.00	26.00
5	Crown	28.00	23.00
6	Edge	26.00	24.00

The measurements from the above tables was then input in a solid modeling program with the correct offsets between each landmark and the simplified geometry created for the rat head. Figure 2 shows this simplified solid rat head.

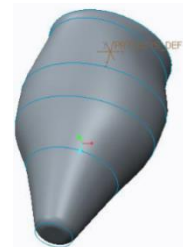


*Figure 2.  
Simplified  
Rat Head*

The head was later investigated for instrumentation placement and is further expounded upon later in this Final Report. Special attention was used to ensure the sensors provide the necessary data to investigate blast wave propagation from the outside of the rat head through the brain and into the rest of the RTD body.

The next step in creating the RTD geometry was to gather information relating to the body of the rat. Some challenges were present in creating a simplified body geometry as the general shape of the rat can vary based on where they carry their weight, much like humans. After some trial and error on taking general measurements at non-descript locations, a method was decided upon using 24 separate rats. These rats were common in age and had approximate masses that were similar. Using this sample size gave confidence that calculating a 50<sup>th</sup> percentile rat geometry from the sample would be accurate.

Landmarks on the body were considered and chosen to ensure that the measurements of each rat would be at the same representative location and make the creation of the database easier. Hand measurements proved to be difficult so a method to capture the geometries and measurements of each rat was created using software. A reference ruler was necessary for the imaging program to determine measurements, so a ruler was designed in CAD and 3D printed.

Each of the 24 rats had two images a piece taken for the software to analyze. The ruler was used as a reference point for the length measurement and the animals were each marked at various landmark locations relating to the skeletal features of the rat. These locations included the base of the neck, the end of the neck, shoulder, last rib, pelvis, thigh, and base of the tail. The lengths between these points were measured and noted and the heights and widths recorded as well.

Taking the raw data from the method above, a normal geometry needed to be calculated. To establish that the data followed a normal distribution, multiple checks of the data were completed. After the 24 data sets were tailed, averaged, and the standard deviation found, a set of cumulative

distribution factors (CDF) were established. The CDFs, along with the mean and standard deviation were used to calculate expected theoretical values and those compared to the observed values. Some outliers were found in this data and removed to create a better average between the theoretical and observed measurements. The before and after outlier removal data can be seen below in Figure 3.

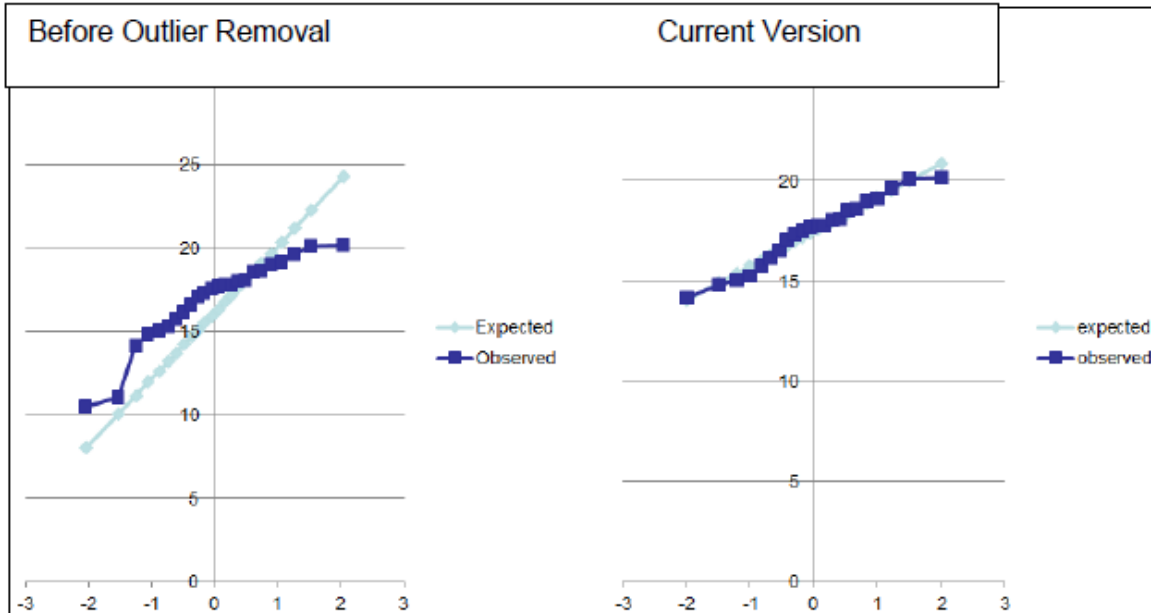


Figure 3. Before and after outliers were removed from measured and expected data

Finally, the 50<sup>th</sup> percentile rat geometry was created from the data sets. Using the inverse normal cumulative distribution, the 50<sup>th</sup> percentile measurements for each point on the rat body were calculated. The measurements created from this calculation are shown in Table 3 below.

**Table 3. 50<sup>th</sup> Percentile Rat Body Measurements**

Position	Length (mm)	between	Height (mm)	Width (mm)
1	17.4365		41.1325	39.10445
2	11.38354		44.10393	43.82494
3	36.85298		47.55217	51.52368
4	44.66971		54.29552	60.61238
5	40.6654		55.96283	69.39611
6	26.01856		50.57267	54.28814
7	n/a		28.73789	23.61623

As with the rat head, ellipses were used in the solid modeling software using the measurements for the 50<sup>th</sup> percentile rat body. Each ellipse was swept with the surface linking them to create one contiguous solid surface. The 2D drawing of this 50<sup>th</sup> percentile rat is shown below in Figure 4. This was the preliminary physical rat geometry moving forward in this project. The drawing

assisted in sensor placement and help plan for manufacturing the prototype.

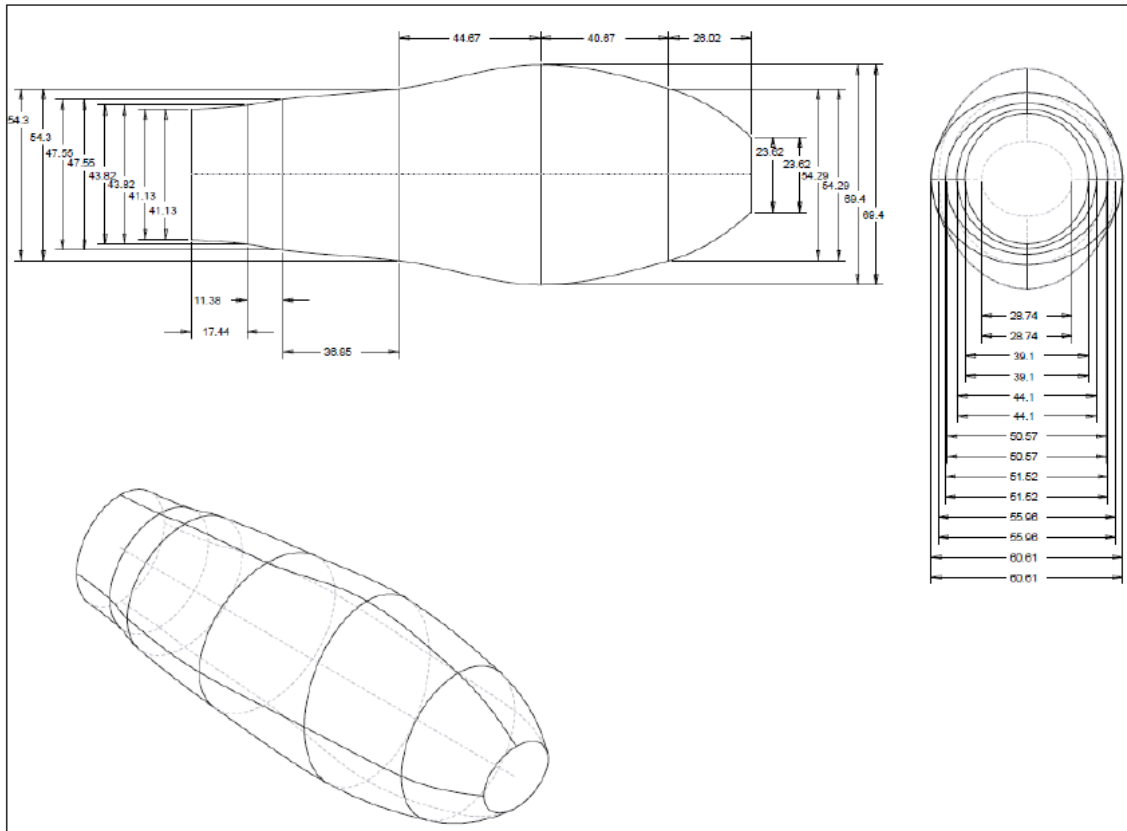
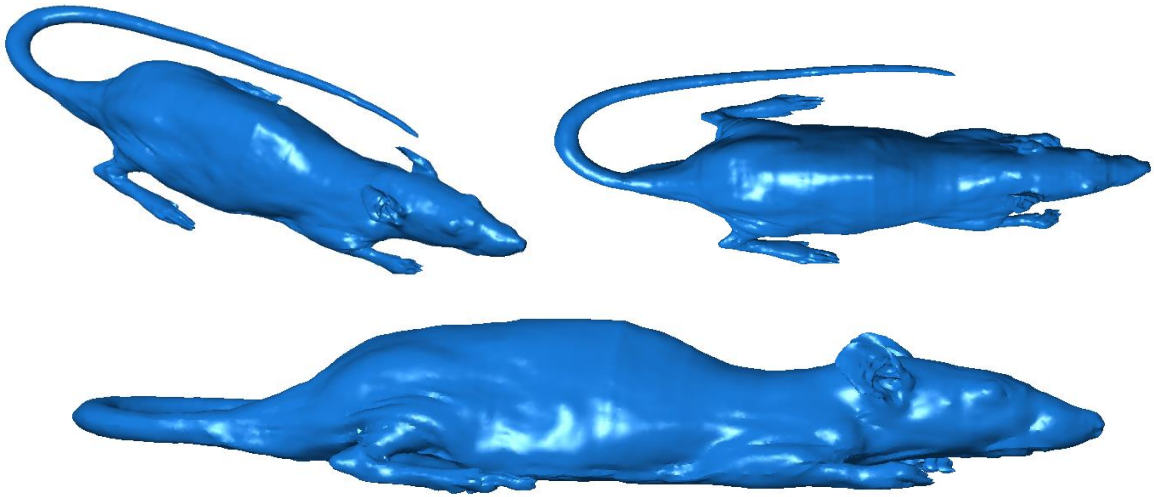
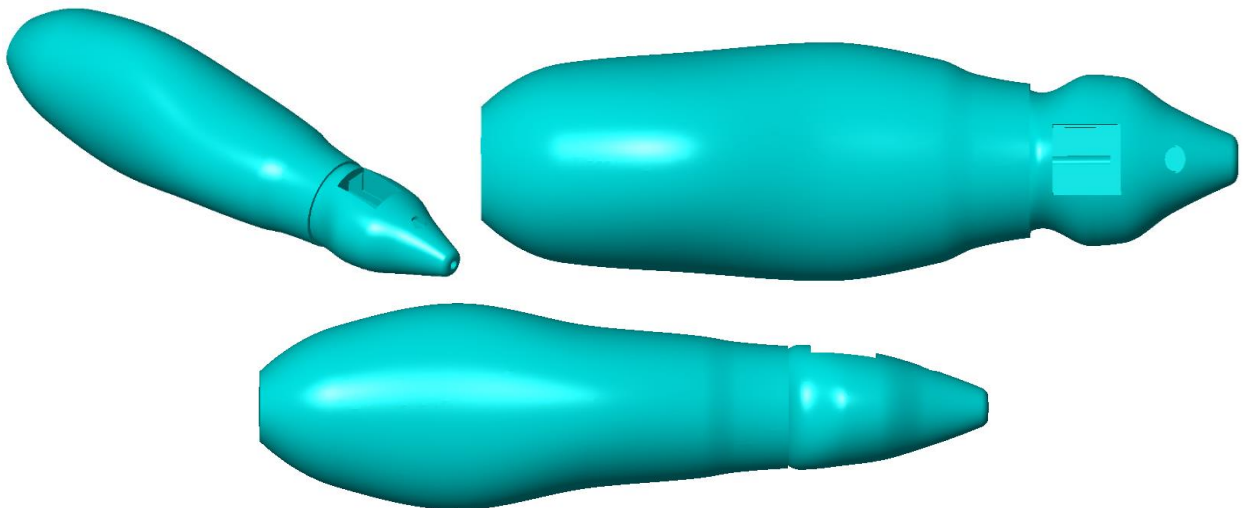


Figure 4. 50<sup>th</sup> Percentile Rat Body 2D drawing with measurements

Next, the non-descript rat surrogate geometry was created from the measurements that represented a 50<sup>th</sup> percentile rat head and body. This rat surrogate was made up of ellipses which sacrificed anatomical accuracy. For this program, the CFDRC/NJIT team took that geometry and correlated it with a more anatomical rat geometry. The starting point for the anatomical rat geometry is shown below in Figure 5.



*Figure 5. Anatomical rat geometry*



*Figure 6. Non-descript rat geometry*

Next, the non-descript geometry was overlaid on the anatomically accurate rat geometry to compare where the anatomical rat could be manipulated to more closely match the 50<sup>th</sup> percentile non-descript RTD design. This overlaid comparison is shown in Figure 7 below.

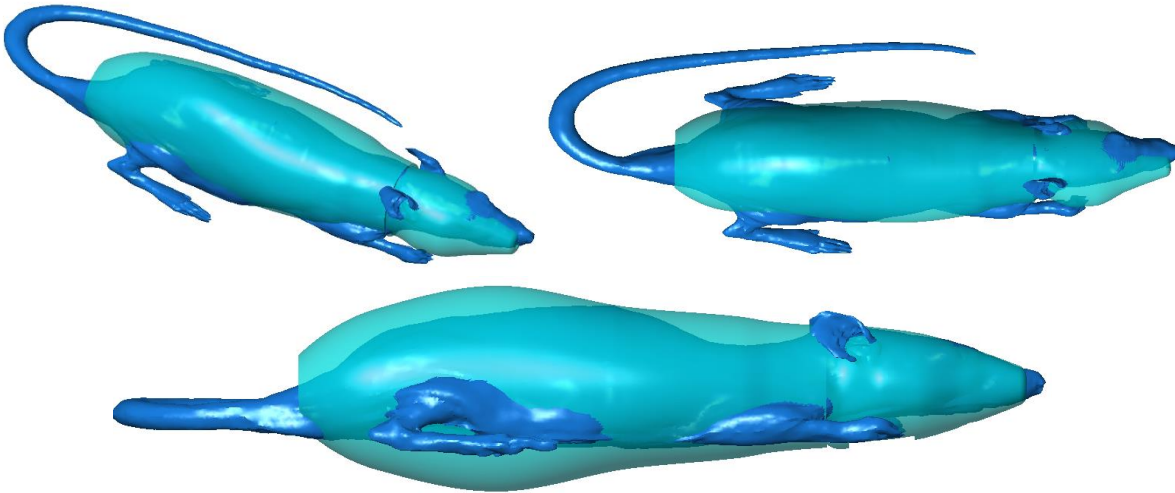


Figure 7. RTD geometry (colored in teal) overlaid on anatomical rat geometry (colored in blue)

Specific areas of improved correlation are the head/neck areas and the posterior areas of the body. As the anatomical rat is flat due to being derived from imaging data, only the upper portion of the rat was matched.

### Task 2. Computational Simulations of Blast Loadings on RTD

CFDRC and NJIT set up a virtual shock tube in CoBi to match simulation results to the past experimental shock tube testing at NJIT. To begin, NJIT sent a detailed schematic of the 9” shock tube that has been used in the previous rat testing. This tube uses helium gas for the driver section which transitions by membrane to a driven section composed of normal air. There is an expansion area after the membrane but before the shock tube transitions into a fully square tube.

## 9” Shock Tube Sensor Location Schematic

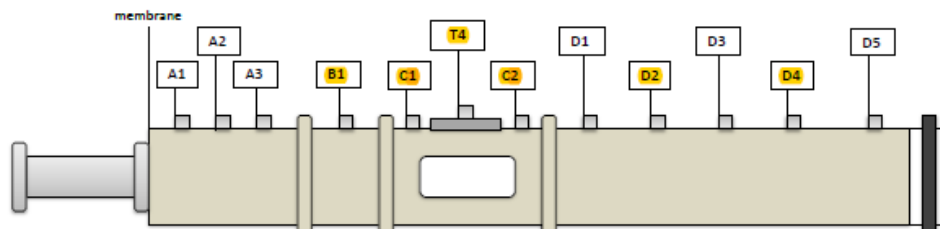


Figure 8. NJIT 9” Shock Tube schematic

Along with the schematic, NJIT provided data on previous empty shock tube tests at 10, 20, and 30 psi which are the levels which will be used on the preliminary prototype RTD developed during this Phase I program. The pressure levels listed correspond to the measurement at the test specimen location which is located where the window is shown in Figure 8 marked by the T4 designation. This is the main pressure location that will be used in setting up the virtual shock tube that will mimic the physical NJIT 9” shock tube. Highlighted in Figure 8 are the pressure

sensor locations that have representative experimental pressure profiles provided by NJIT. This allowed further validation and correlation with the virtual shock tube. One experimental test was picked as a starting point for correlating the data as a baseline for the virtual shock tube. The information for that run is shown below in Table 4.

**Table 4. Experimental Shock Tube Parameters for 10 psi test**

Barrel Length	9 inches
Breech Length	21.75 inches
Driver Gas	Helium
Ambient Temperature	75.49 °F
Barometric Pressure	14.4 psia
Burst Pressure	80.12 psi

Figure 9 shows the pressure data from the six pressure sensor locations.

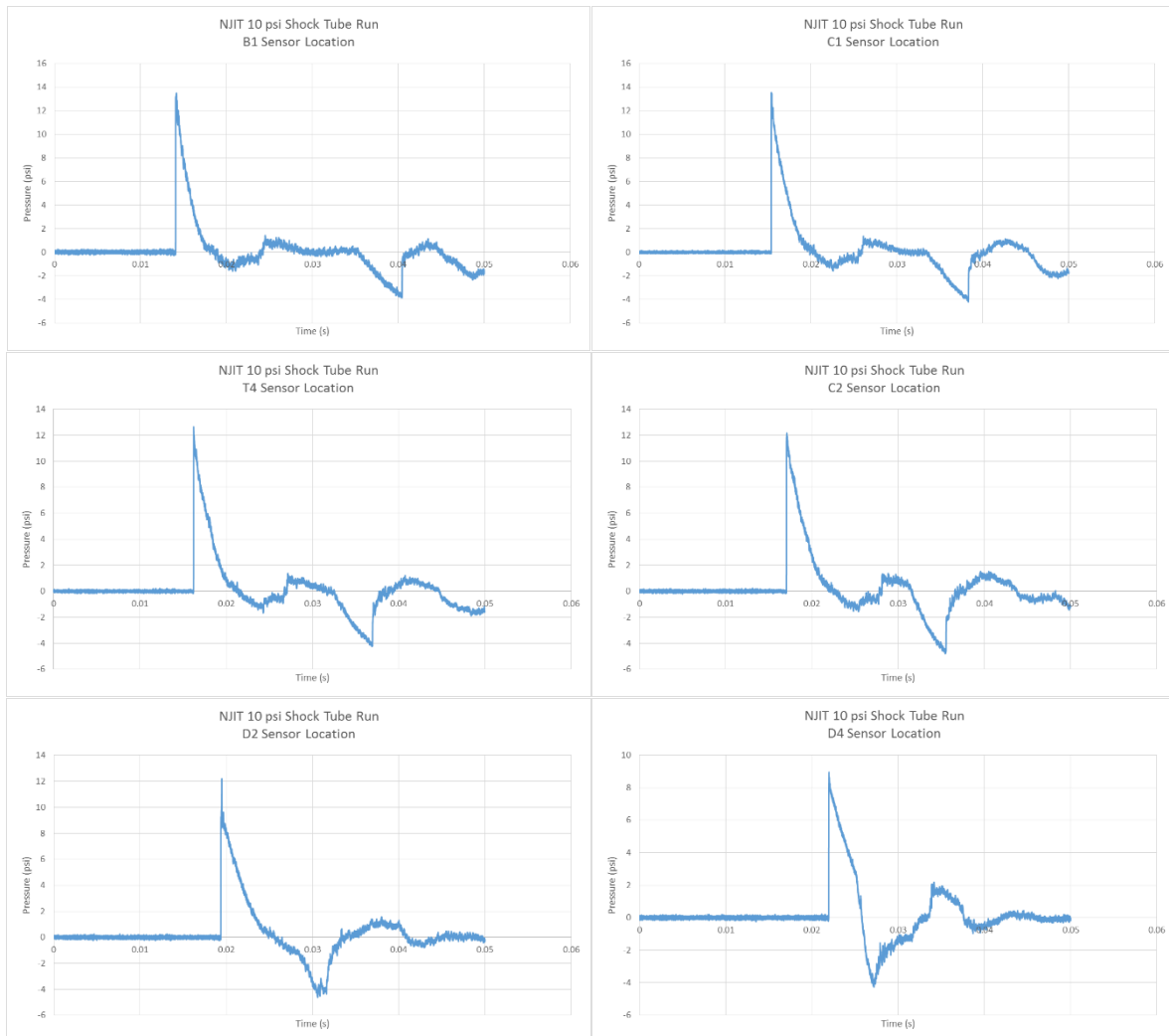


*Figure 9. Experimental shock tube pressure traces for 10 psi target exposure (at various locations)*

While data is recorded at many locations along the tube, the critical area of matching between the experimental values and the simulations is the sensor located at T4. This location is the middle of the specimen area where the rigid RTD will be placed in future experiments during this program. To simulate the loadings on the RTD in a simulation environment, close matching at this sensor was used to verify and validate the simulation framework developed in CoBi. Figure 10 shows the pressure data of the sensor located at T4 for the experimental run that is described above.

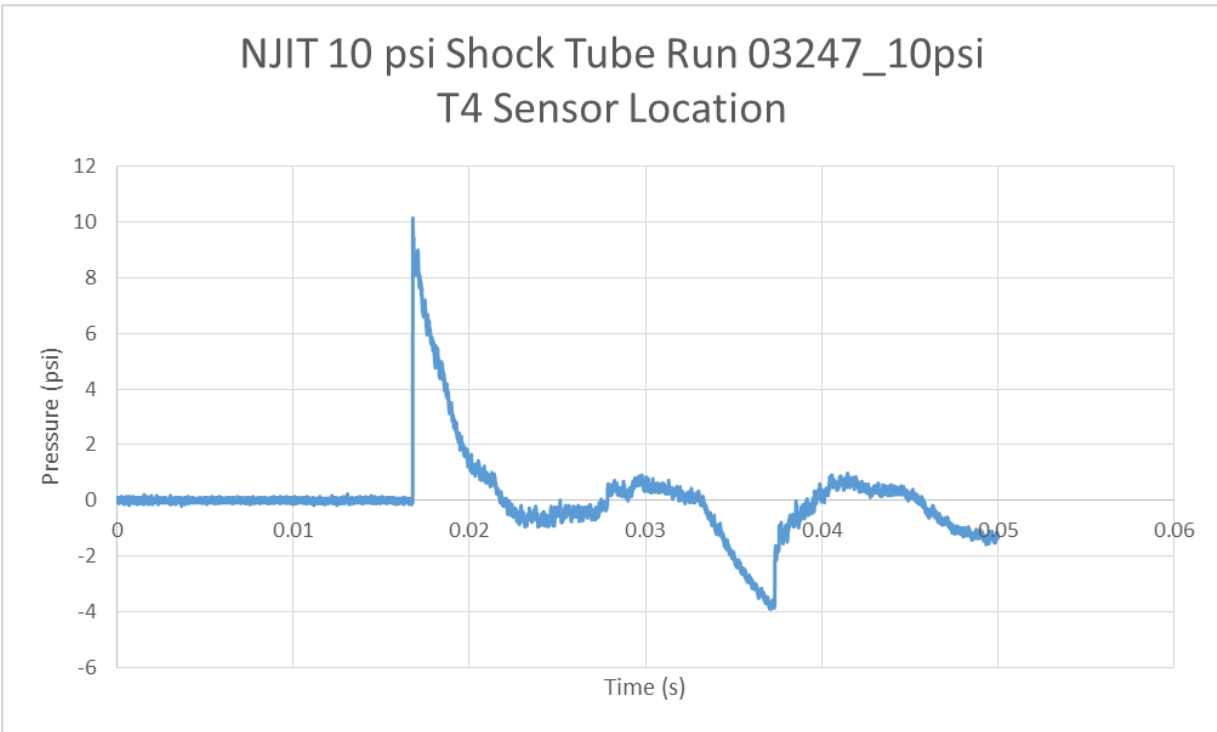


Figure 10. Experimental shock tube pressure traces for 10 psi target exposure (at T4 location)

In this program, the CFDRC/NJIT wanted to use multiple approaches (1D/3D, CoBi wire, CoBi structured mesh) as part of a combined framework for the simulation/experimental validation and matching of the shock tube at NJIT. This combined approach allows for a wide variety of investigations on the future RTD. A virtual shock tube geometry that matched the NJIT shock tube was created in CFD-GEOM. This discrete surface geometry allows for a wireframe to be built off the measurements given by NJIT. Figure 11 shows a simple schematic derived from the measurements of the 9” NJIT and Figure 12 shows the shock tube recreated in CFD-GEOM.

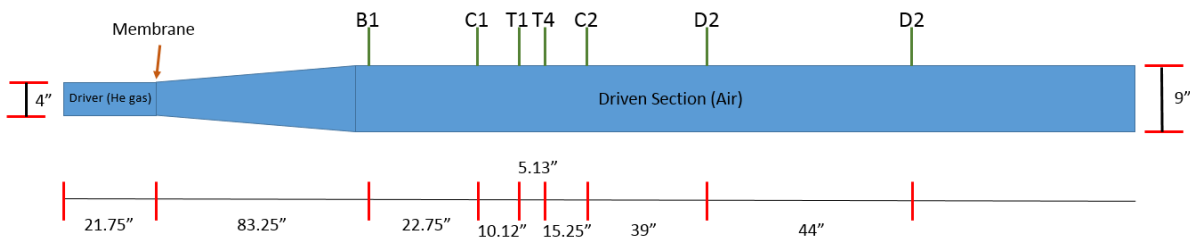


Figure 11. Virtual schematic of the NJIT 9” shock tube with pressure sensor location offsets

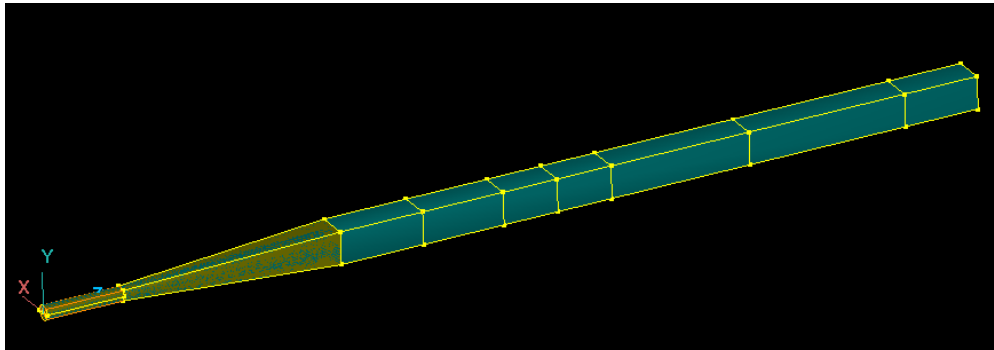


Figure 12. 3-D model of NJIT 9" shock tube in CFD-GEOM before meshing

Next, a structured mesh with approximately 700K cells was created from the surfaces shown in Figure 12. The structured mesh includes the driver section which is modeled with compressed helium gas and the driven section which contains ambient air. Figure 13 below shows this structured mesh. The top image shows the shock tube walls and the bottom image shows the one driver volume and four driven volumes.

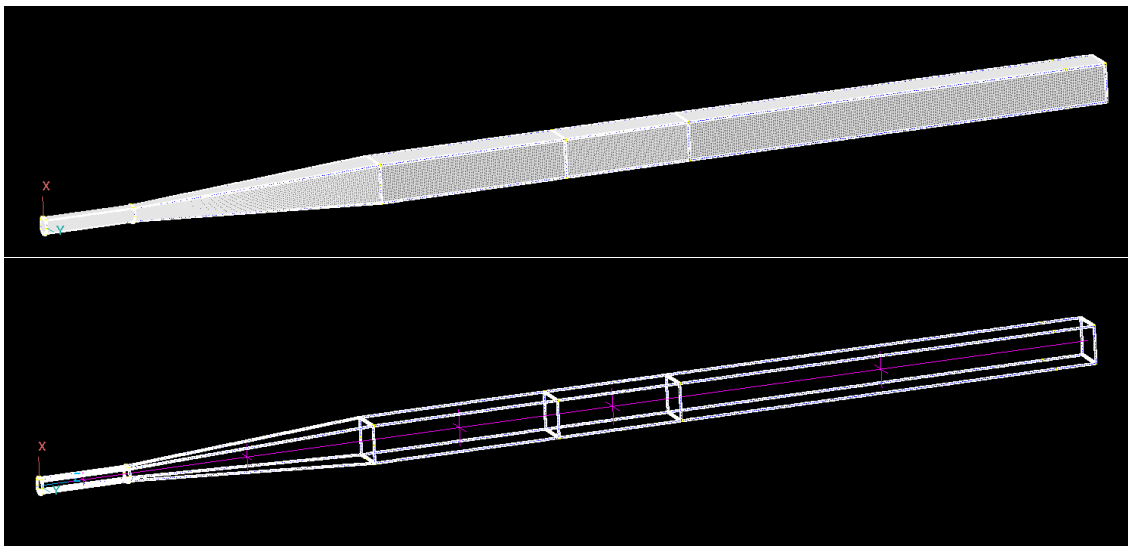


Figure 13. Structured mesh in CFD-GEOM representing the 9" NJIT shock tube

In later experiments, the RTD was placed in the test specimen area of the 9" shock tube where the T4 sensor is placed. This location was used to tune the virtual shock tube and create a close matching between experiments and simulations. To start this verification process and as part of the multiple approach to creating a simulation framework, a CoBi wire model was used to set-up virtually the same shock tube in a simplified and reduced cell count simulation. CoBi solves laminar flows including incompressible and compressible flow. The compressible flow here means compressible gas flow with idea gas law with multi idea gas components. The following are governing equations.

Mass conservation equation (continuity equation):

$$\frac{\partial \rho}{\partial t} + \frac{\partial \rho u_j}{\partial x_j} = S_m \quad (1)$$

where  $\rho$  is idea gas or idea gas mixture density,  $u_j$  is the velocity vector and  $S_m$  is the mass source term.

Momentum conservation equation (Navier Stokes equations):

$$\frac{\partial \rho u_i}{\partial t} + \frac{\partial}{\partial x_j} \rho u_j u_i = -\frac{\partial p}{\partial x_i} + \frac{\partial \tau_{i,j}}{\partial x_j} + F_i + S_{u_i} \quad (2)$$

where  $p$  is the static pressure,  $\tau$  is the stress tensor (described below),  $F_i$  presents the body force e.g. gravity force or frictional force in porous media (described below). The first term is the momentum rate change, the second term is the convection term, on the right hand side the first term is the pressure driving term, the second term is viscous shear stress term. The viscous stress tensor  $\tau$  is

$$\tau_{i,j} = \mu \left( \frac{\partial u_i}{\partial x_j} + \frac{\partial u_j}{\partial x_i} \right) - \frac{2}{3} \mu \frac{\partial u_k}{\partial x_k} \delta_{i,j} \quad (3)$$

where  $\mu$  is the fluid molecular dynamic viscosity.

Energy equation:

$$\frac{\partial \rho H}{\partial t} + \frac{\partial}{\partial x_j} \rho u_j H = \frac{\partial}{\partial x_j} k \frac{\partial T}{\partial x_j} + \frac{\partial}{\partial x_j} u_i \tau_{j,k} \delta_{i,k} + \frac{\partial p}{\partial t} + S_H \quad (4)$$

Where,  $H$  is total enthalpy,  $k$  is conductivity,  $S_H$  is additional source and  $\delta_{ij}$  is defined as

$$\delta_{ij} = \begin{cases} 1, & i = j \\ 0, & i \neq j \end{cases}$$

Species transport:

$$\frac{\partial \rho c_i}{\partial t} + \frac{\partial}{\partial x_j} \rho u_j c_i = \frac{\partial}{\partial x_j} \rho D_i \frac{\partial c_i}{\partial x_j} + S_{c_i} \quad (5)$$

where  $S_{c_i}$  is the net rate of production specie  $c_i$  by chemical reaction,  $D_i$  is the diffusivity of species  $i$ . The source  $S_i$  can be obtained by coupling a general ODE solver within CoBi.

Ideal Gas Law:

$$p = \rho R_u T \sum_{i=1}^N \frac{Y_i}{W_i} \quad (6)$$

Where,  $R_u$  is the universal gas constant,  $Y_i$  is the mass fraction of  $i^{\text{th}}$  gas component and  $W_i$  is the molecular weight of the  $i^{\text{th}}$  gas component. For pure air, equation (6) becomes

$$p = \rho \frac{R_u}{W_{air}} T \quad (7)$$

Where  $W_{air}$  is the air molecular weight (=28.9 g/mole K).

### 1D-3D Mix Simulation

CoBi has a built-in technique that can handle flow simulation between 1D to 3D mesh connection, which CoBi names as “link face” shown in Figure 14. The connection ends for each grid can be tight linked or separated in space.

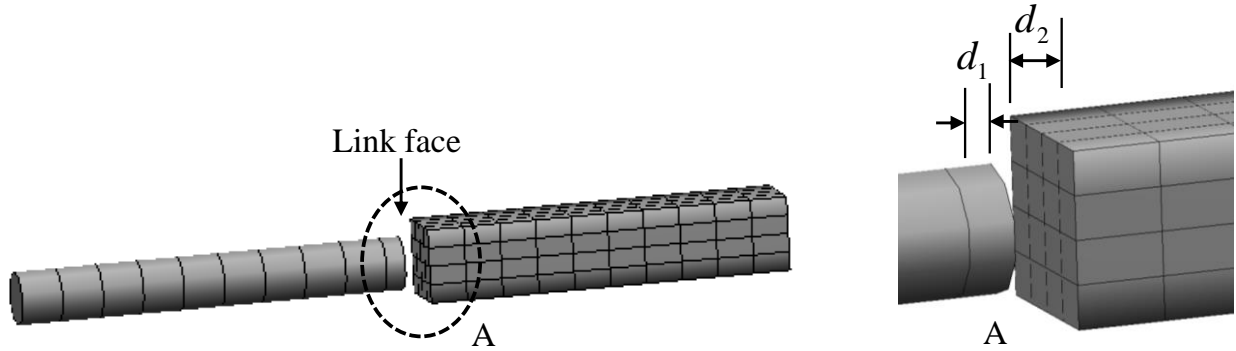


Figure 14. 1D to 3D mesh linking

CoBi assigns equal mass flux, thermal flux and species flux, from one end to another end and calculate average value at the link face for any quantity,  $\phi$ , such as pressure, velocity, temperature, and species concentration as following:

$$\bar{\phi} = \varepsilon \phi_{left} + (1 - \varepsilon) \frac{\sum_{i=1}^n \phi_{right,i} A_i}{\sum_{i=1}^n A_i} \quad (8)$$

Where,  $A_i$  is the cell face area at the right 3D grid at link face and  $\varepsilon$  is geometry related distance

function defined as

$$\varepsilon = \frac{d_1}{d_1 + d_2} \quad (9)$$

$d_1$  and  $d_2$  is half cell distance between cell center to cell face at link face. Figure 15 shows an example testing simulation result of pressure and velocity in channel flow.

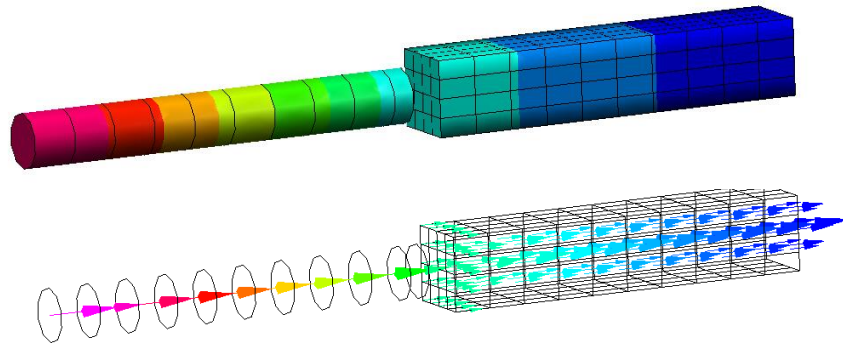


*Figure 15. Example of flow pressure (top) and velocity vectors colored by pressure (bottom) in 1D to 3D mixed grid.*

The technique of 1D to 3D link face connection in CoBi provides a great capability to handle complicated geometry and capture detailed flow characteristics as required for certain critical areas. For a non-critical areas, we can use 1D mesh and for any critical area we can use 3D detailed mesh. This technique saves a lot of simulation time.

In blast experiments using shock tubes, the configuration at the end of the shock tube dictates what the blast curve looks like after the initial positive impulse wave followed by the expansion wave which has a slight negative pressure dip. NJIT's shock tube uses an offset reflector plate located 2 inches off the open end of the shock tube. For simulation matching, we are only concerned about the initial positive impulse phase and the negative expansion wave phase that follows the positive phase as past work has shown this to be the most critical injury cause relating to blast. In real world blast events, there is no reflected wave from the outside environment, unless inside a structure and then the reflected waves have a different signature. The area of interest in the experimental data is shown below in Figure 16 below.

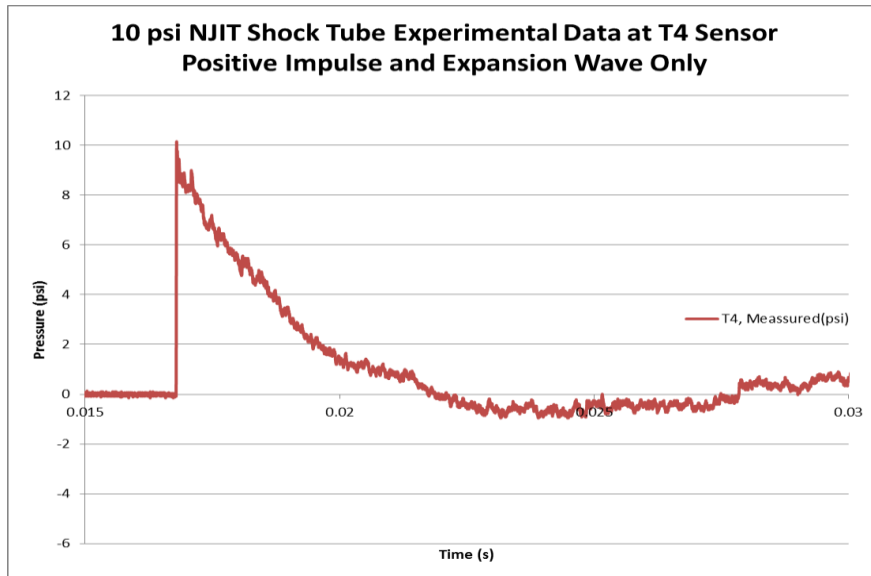


*Figure 16. 10 psi NJIT shock tube data at T4 sensor*

Next, a 1D wire simulation was created to quickly iterate through the various parameters necessary to match NJIT’s experimental shock tube results. The confidence level of the burst pressure measurement is not high due to the quick fill and bursting of the membrane. To match the downstream pressure, an iterative approach was used to adjust the burst pressure of the helium filled driver section in the 1D wire model simulation. After a few iterations, a good agreement was reached using the CoBi framework. The results of the 1D wire model run are shown below in Figure 17.

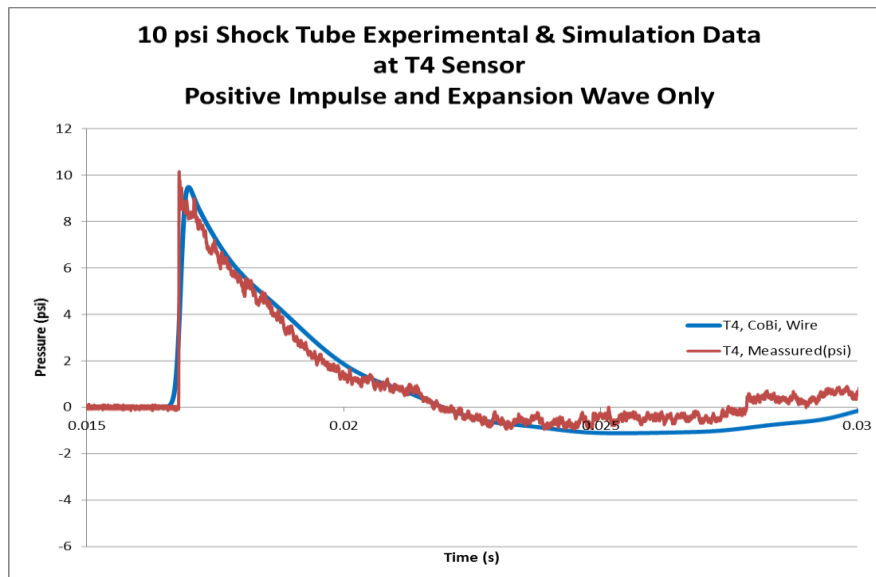


*Figure 17. Experimental & 1D CoBi wire model comparison*

### Task 3. Design Specifications for RTD (Sensors, Materials)

The initial design idea of the rodent testing device (RTD) relies almost solely on the proper implementation of the shape factor, which mimics to a large degree the anatomy of the rodents used most frequently in the shock tube/field experiments. This emphasis stems from the limitation of the existing studies where a variety of exposure conditions, shock tube designs, animal orientations and variety of animal models obscures the interpretation of the results. These factors combined with inadequately defined reporting standards render all existing literature very difficult to interpret, and translation of findings into the clinical area next to impossible. The device aimed at standardization of exposure conditions and reporting is thus a necessity to advance the field. Successful implementation of the design requirements for the device calls for the implementation of the modular system with four independent components:

1. Geometrical model
2. Pressure sensors and accelerometer
3. Data acquisition sub-system (hardware)
4. Data acquisition and analysis sub-system (software)

Considering the development of components 3 and 4 will require substantially more effort than the design of the geometrical model, there are several factors to seek the expansion of the applicability of the system. Deployment of the system to laboratories interested in pressure measurements other than animal testing would require only minor modifications to the design of the geometrical model and would greatly expand the economics of the project and potential market. Economics is a strong incentive to treat this project as a general pressure measurement system rather than a product addressing a niche application with limited deployment options. This change in the design approach is inclusive of the original goals of the project and did not jeopardize in any way the original scope of the project. It was oriented towards the maximal utilitarian value of the platform and recognizes its usability in a much broader context and represents a strong commitment by the design team towards successful completion of the product.

The implementation of the modular design with this broader outreach perspective considered many factors like incorporation of the sensors available on the market into our product, certification that certain sensors are suitable to operate properly with the device, supply necessary accessories facilitating attachment of specific class of sensors, and ensure measured pressures are accurate representation of the reality. The modular vision for the system will help expand the client base accommodating their specific requirements regarding the shape of the probe and facilitating the choice of sensors addressing their measurement requirements, e.g., pressure range and sensitivity.

### Task 4. Fabricate the RTD

The CFDRC/NJIT team generated a CAD drawing of the reduced fidelity body model. The model was designed as a two-part assembly to investigate the feasibility of the sensor mounting, aerodynamics of the enclosure and possible effects associated with the two-shell assembly on the pressure distribution. We have added modifications to the model in lieu of the experimental requirements for shock tube and field testing:

- the flat bottom to facilitate the model mounting
- mounting screws openings for quick access inside of the prototype

- three sensor mounting ports designated to accommodate the PCB 102B06 sensors

The CFDRC/NJIT team produced the low density, thin wall RTD prototype made of polylactic acid (PLA) polymer using 3-D printing methodology. The prototype was used to initially evaluate and optimize the options for the sensor mounting and prototype attachment in the shock tube, and to evaluate the selection of the cut lines dividing the model into two-part assembly. Figure 18 shows the exterior of the RTD prototype.



*Figure 18. Exterior overview of the assembled RTD prototype*

Figure 19 shows the interior of the RTD prototype with pressure sensors and wiring.



*Figure 19. Interior overview of the RTD prototype showing sensor mounting and wiring*

This preliminary prototype was rough and not fully smoothed after 3D printing. The first priority was getting the sensors mounted correctly and the wiring routes laid out before further sanding and finishing the RTD.

The evaluation based on the preliminary 3D printed prototype resulted in an updated list of specifications for further refinement of the device. The CFDRC/NJIT team noted the following limitations of that preliminary RTD model:

1. The size of the 102B06 sensors makes them less suitable candidates to meet the selection criteria of the project. It is unlikely we can accommodate these sensors in any preselected positions in the model. The 10-32 mounting nut to attach the low noise signal cable and the cable stiffness would require much more space than the RTD body can offer without the potentially detrimental necessity to bend the cables.
2. Considering the limitations of the 102B06 sensors, we have opted to use smaller sensors and the PCB model 132B38 micro ICP<sup>®</sup> pressure sensors. The size of these sensors (OD

0.125 in., their response time ( $<1 \mu\text{s}$ ) and pressure range (50 psi) make them good candidates for the RTD. These sensors are also readily available from the manufacturer, unlike other similar solutions (e.g. Kulite XCL-072 series), which have limited availability and lengthy lead time (up to 6 months) with no price advantage (\$700 PCB vs \$800-\$1200 Kulite, depending on the sensor model).

3. The diagonal slit will be moved to the bottom part of the RTD model for better aerodynamics, and we are also going to perform sensor mounting adjustments to accommodate new miniature sensors from PCB.
4. The volume of the next generation CAD drawing of the RTD with all the sensors will be adjusted to match the weight of 350 g. This is necessary to meet the body mass of the 10 weeks old Sprague Dawley rat, and facilitate the testing of the RTD in an unrestrained configuration.
5. The RTD will be mounted in the shock tube using a quick release adapter plate attached to the electromagnet and a clip attached to the body of the RTD. This will eliminate the use of the designated mounting plate adapter for a specific shock tube configuration.
6. The switchable electromagnet base will permit pressure measurements in any location in the shock tube offering great degree of flexibility. To the best of our knowledge this solution has not been used in this type of testing before.

Notable purchases during the program:

- PCB model 132B38 micro ICP pressure sensors, 5 e. a.
- portable USB DAQ from NI (NI USB-6212), 1 e. a.
- Tripod Quick Release Adapter for Mounting the RTD (with B-Grip Adapter Plate)
- Quick Release Plate (for mounting the RTD)

A new version of the RTD was printed during later in the program to house the micro ICP sensors. This new design is more aerodynamic and closer to matching the shape of an anatomical rat while still providing good mounting areas for static and dynamic pressure measurements. This RTD design and sensor layout was used for the preliminary shock tube testing. Figure 20 shows the RTD with sensors and placed in the specimen area of the shock tube.

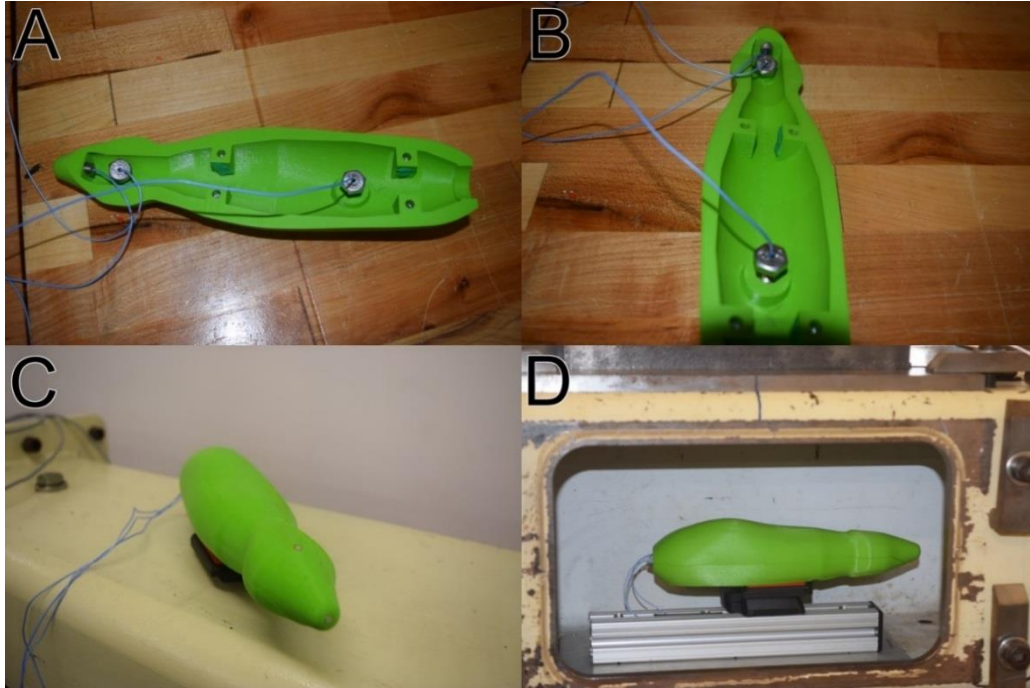


Figure 20. The shock tube testing of the latest version of the RTD. Details of the sensor location and wiring (A, B), the assembled model (C), and the instrumented model mounted in the shock tube (D).

#### Task 5. Experimental Testing of the RTD

The updated model of the RTD was 3D printed and instrumented with three micro ICP<sup>®</sup> pressure sensors (PCB Piezotronics, 132B38). The advantage of these sensors over the other smallest available pressure sensors that PCB offers (ICP<sup>®</sup>102B06) is their smaller size, which makes them the most suitable for the implementation in a confined space of the frontal part of the model. The PCB 102 series has been used widely in the past in the shock tube testing at NJIT and have proven reliable over hundreds of tests without any issues or failures. However, this is the first time that the micro pressure sensors, 132B38, have been used. Unfortunately, all five ordered sensors suffer from issues which initially prevented them from acquisition of accurate pressure profiles.

These sensors have two leads and the all possible combinations of wiring were evaluated, including tests where these sensors were connected to the signal conditioner and with the sensor by-passing the signal conditioner. The PCB support was notified about these issues and work continued to diagnose the problem. The testing configuration is shown below in Figure 21.

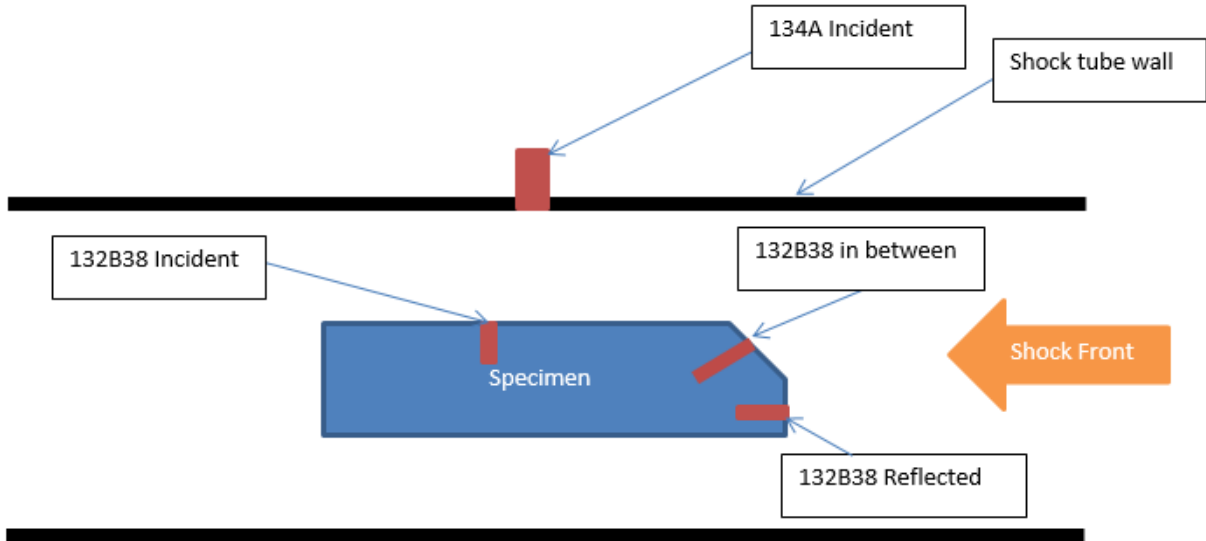


Figure 21. Experimental Shock Tube testing set-up with new micro ICP sensors in RTD

The data from the testing is shown below.

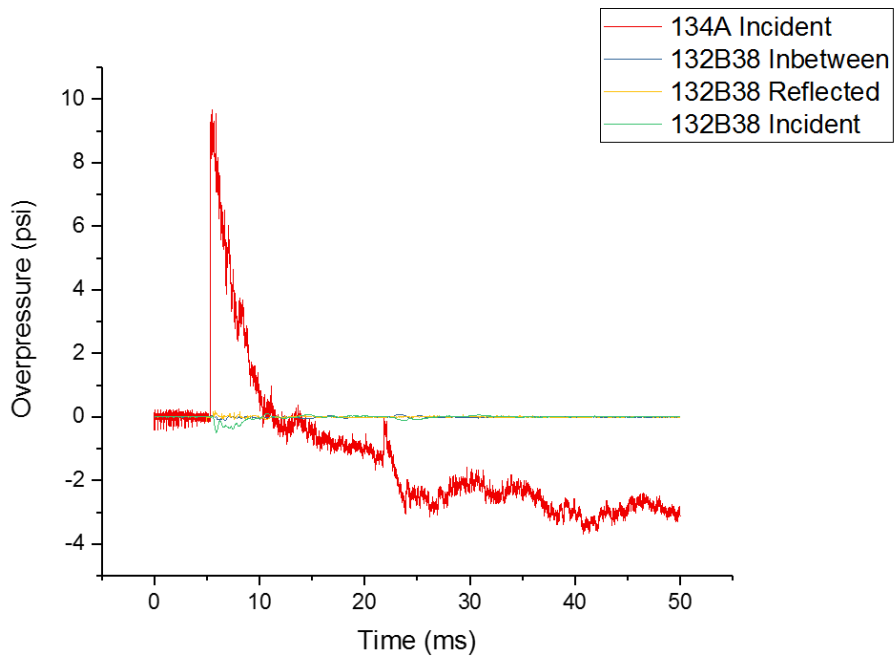


Figure 22. The test experiment at nominal shock wave intensity of 10 psi (134A sensor). Micro ICP sensors were connected by-passing signal conditioner using the polarity from product manual (black lead (+), silver lead (-)).

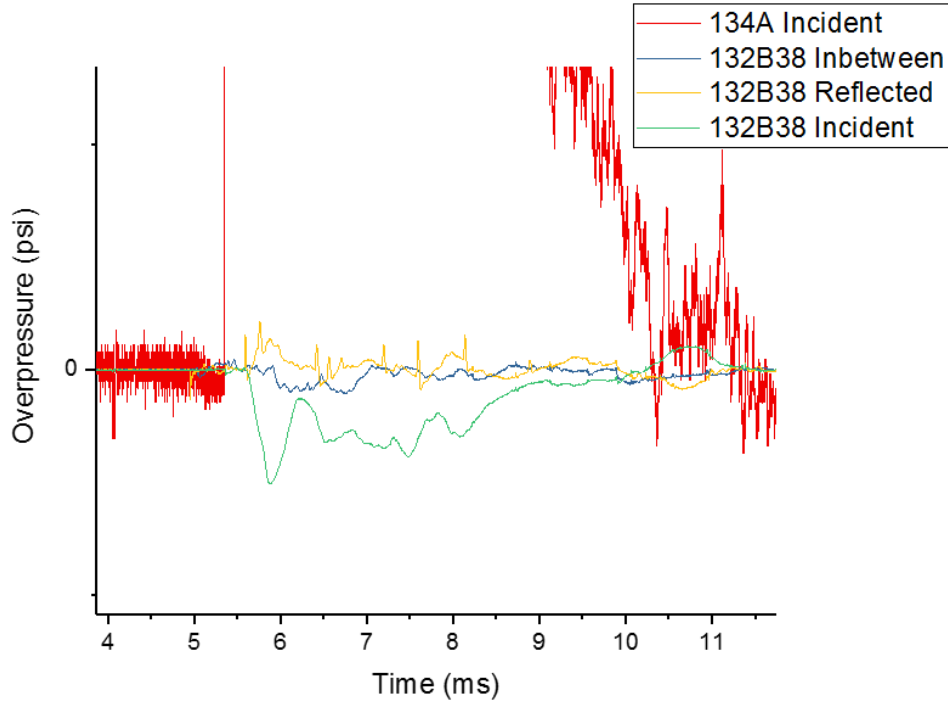


Figure 23. The test experiment at nominal shock wave intensity of 10 psi (134A sensor). Micro ICP sensors were connected by-passing signal conditioner using the polarity from product manual (black lead (+), silver lead (-)).

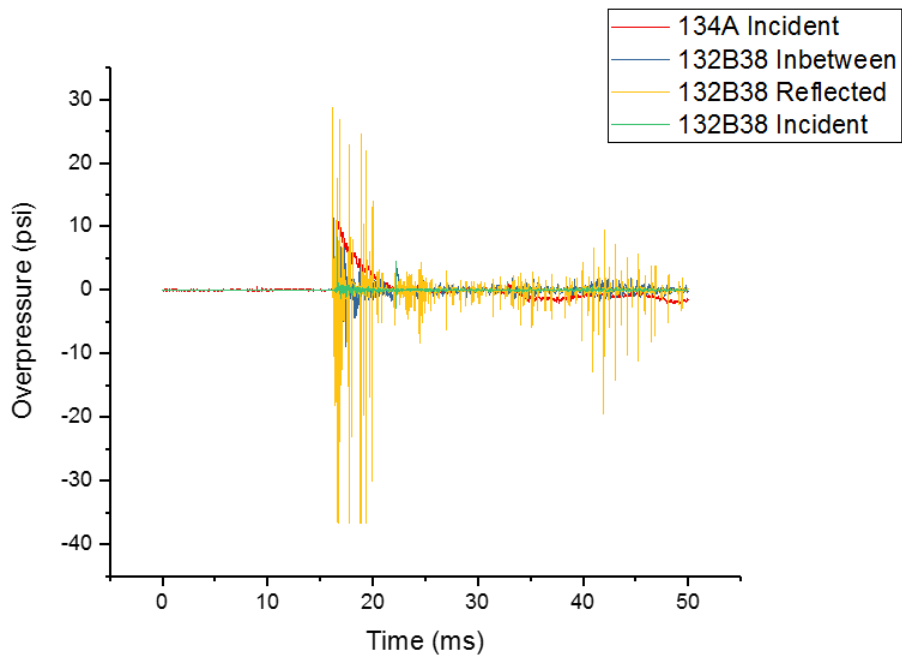


Figure 24. The test experiment at nominal shock wave intensity of 10 psi (134A sensor). Micro ICP sensors were connected via signal conditioner using reversed polarity (black lead (-), silver lead (+)).

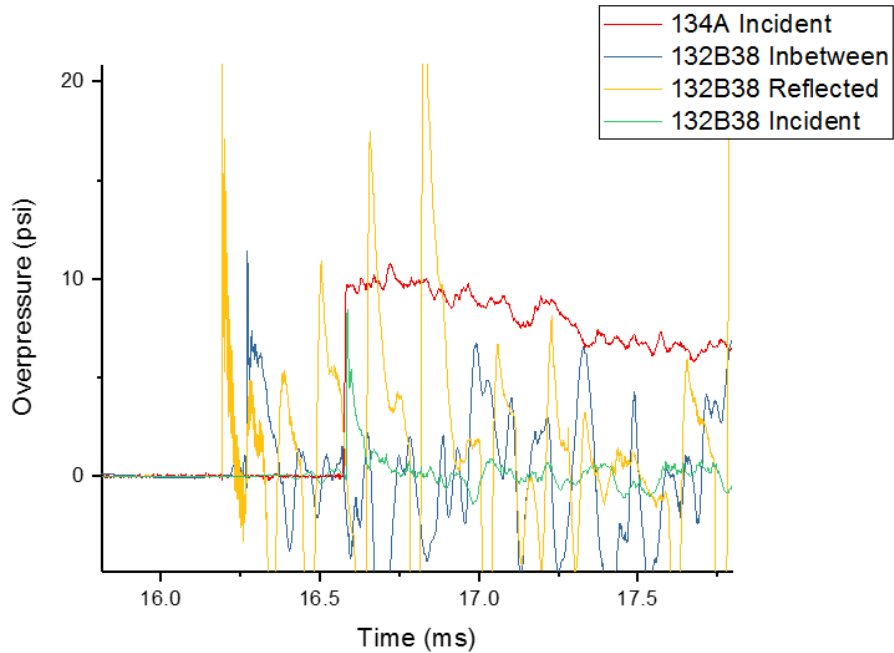


Figure 25. The test experiment at nominal shock wave intensity of 10 psi (134A sensor). Micro ICP sensors were connected via signal conditioner using reversed polarity (black lead (-), silver lead (+)).

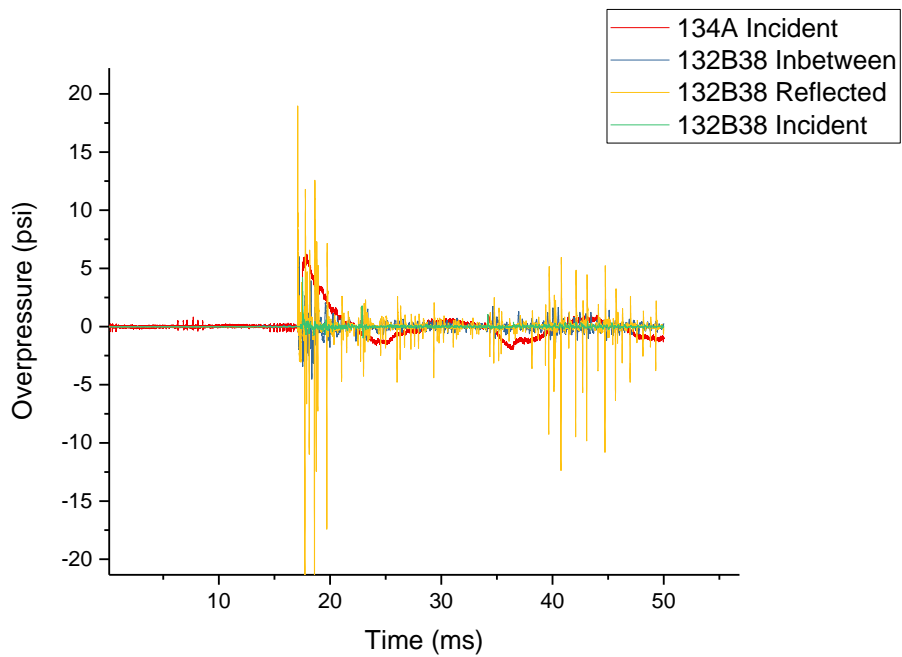
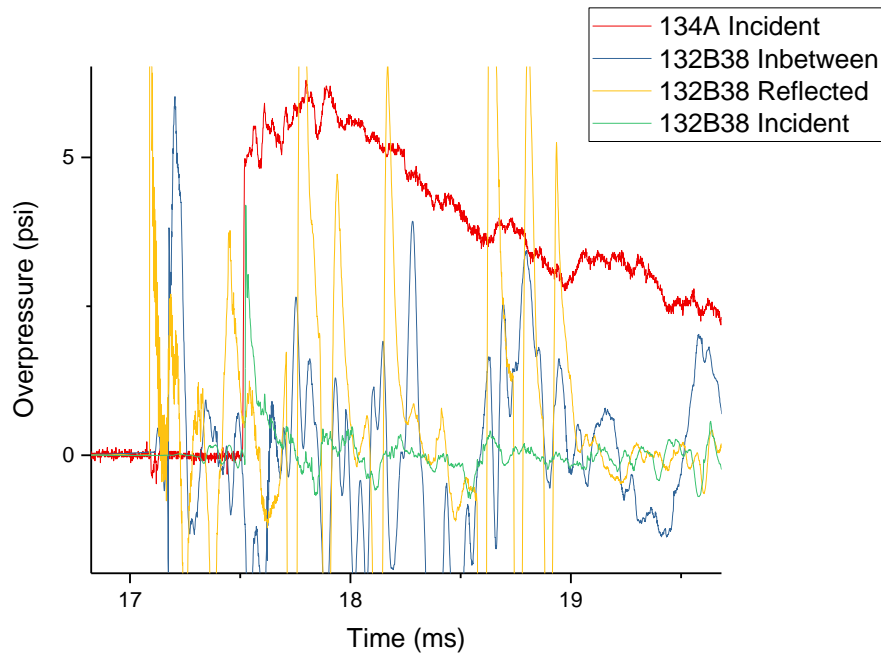
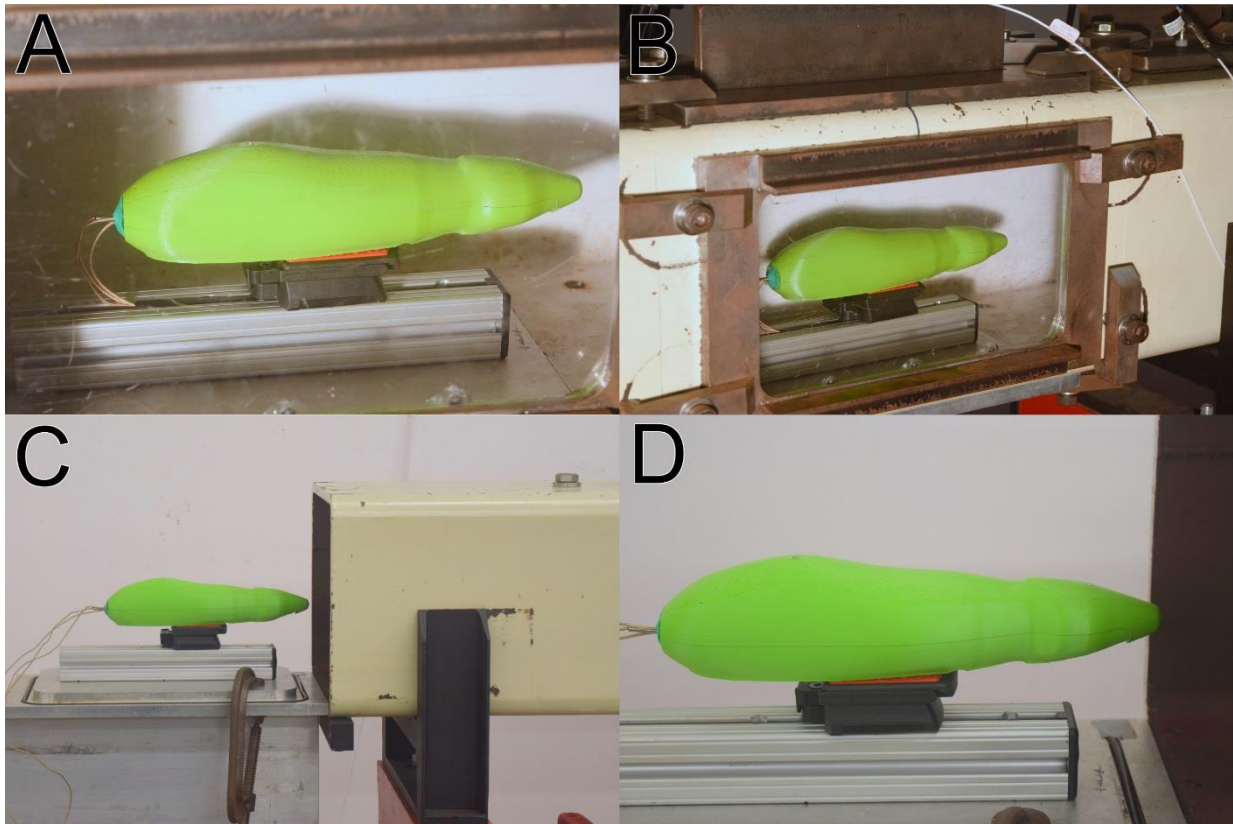


Figure 26. The test experiment at nominal shock wave intensity of 5 psi (134A sensor). Micro ICP sensors were connected via signal conditioner using reversed polarity (black lead (-), silver lead (+)).



*Figure 27. The test experiment at nominal shock wave intensity of 5 psi (134A sensor). Micro ICP sensors were connected via signal conditioner using reversed polarity (black lead (-), silver lead (+)).*

The next iteration of the preliminary high-density 3D printed model was instrumented with three pressure sensors: one PCB 102B06 mounted in the snout location (this pressure sensor will measure the total pressure), and two miniature Kulite sensors (XCL series) in the forehead and back locations. The forehead sensor is mounted at 20° incident angle with respect to the axis of symmetry of the model, and the back sensor is mounted at 90° with respect to the axis symmetry. These sensors were used to measure the surface pressures at three nominal shock wave intensities: 70, 130 and 180 kPa in two different locations: in the inside of the shock tube (fig. 2A, B) and on the outside (fig. 2C, D).



*Figure 28. The 3<sup>rd</sup> generation 3D printed RTD prototype instrumented with three pressure sensors during the shock tube testing. The prototype is mounted in the inside (A, B) and outside locations (C, D).*

The representative pressure profiles recorded by the incident (side-on) pressure sensor in the T4 location inside of the shock tube, and three pressure sensors mounted in the body of the RTD prototype are presented in Figure 29 and Figure 30. As expected, the profiles are different for the inside versus outside test locations. The duration of the pressure pulse is markedly reduced in the outside location, which results in reduced impulse values for the outside test location. This is expected outcome and demonstrates the device can be used to distinguish between different test locations, where the flow dynamics varies significantly. The shock waves of varying intensity are also easily detectable with the application of the RTD (the intensity of these shock waves lies in the typical range used in the laboratory tests performed by researchers involved in the etiology of blast TBI). It is worth to note, that an incident pressure profile (T4) is replicated at lower pressures by the “Back” sensor, but the discrepancy exists at higher nominal pressures. The shape factor might be responsible for observed discrepancies. This is an important observation considering the RTD in a standalone configuration will be used to determine the loading conditions. The simple correlation between the recordings of sensors mounted in the RTD and incident pressure is sufficient to overcome this limitation of the prototype. End users should be supplied with calibration tables depicting pressure gradients at different standard test locations.

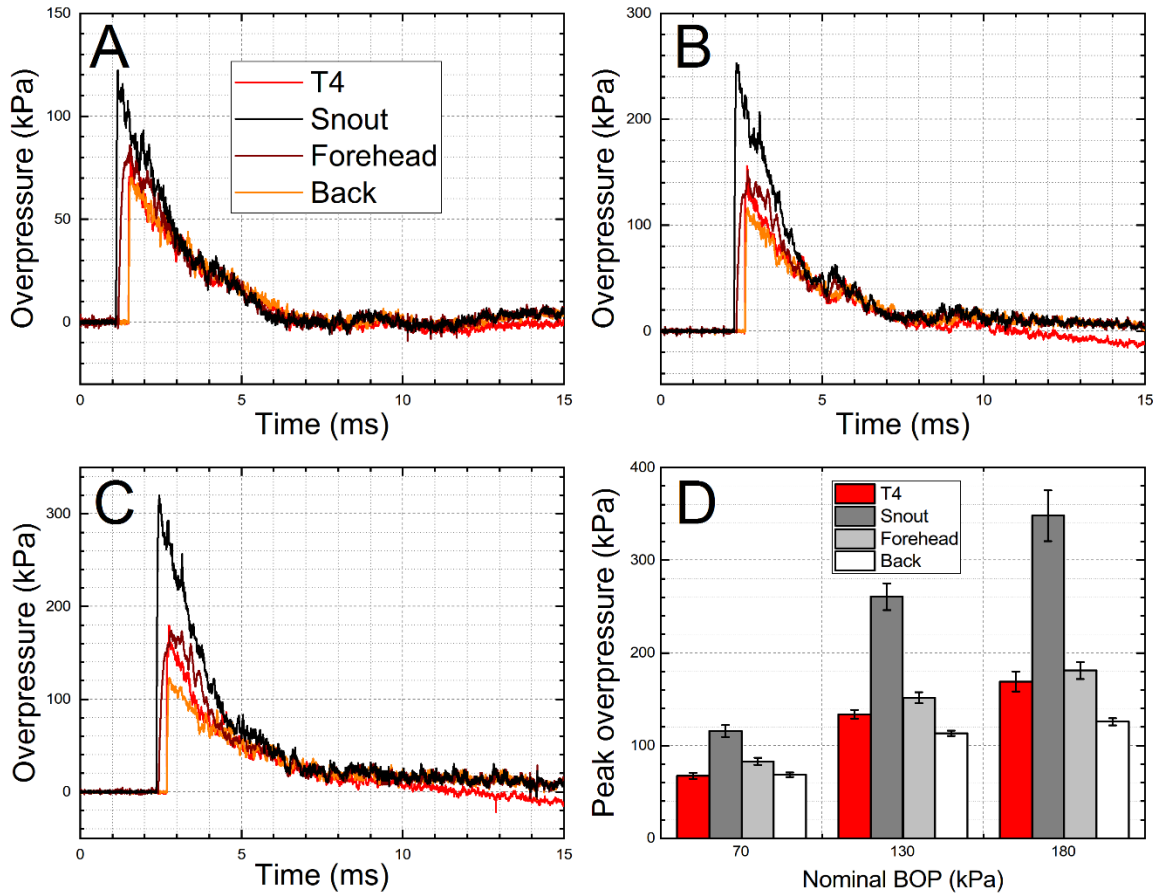


Figure 29. The RTD testing in the shock tube: inside location. The representative pressure profiles recorded by the incident pressure sensor (T4) mounted in the shock tube wall, and three pressure sensors mounted in the RTD prototype and exposed to a single shock wave with nominal intensity of: A) 70 kPa, B) 130 kPa, and C) 180 kPa. The quantification of the peak overpressure values is presented in figure D. Tests were repeated four times at each nominal shock wave intensity.

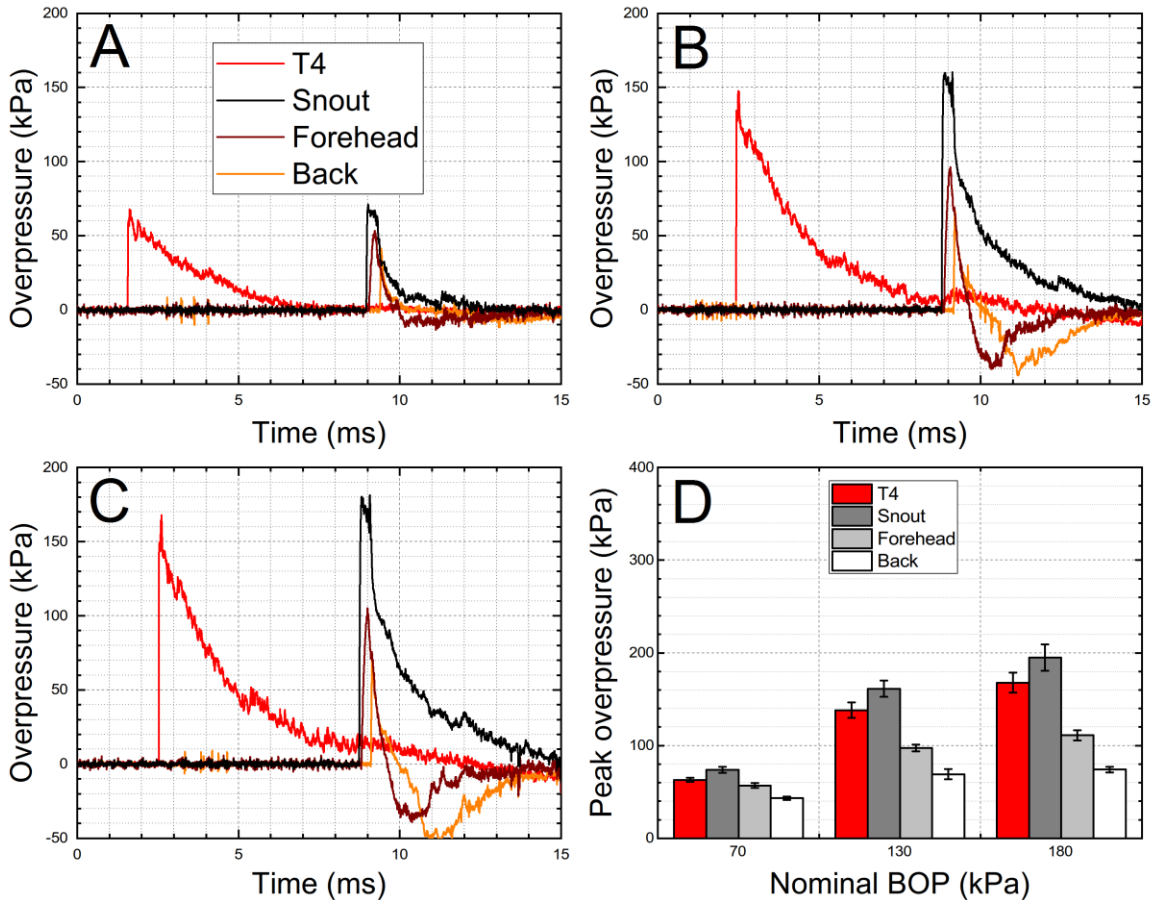
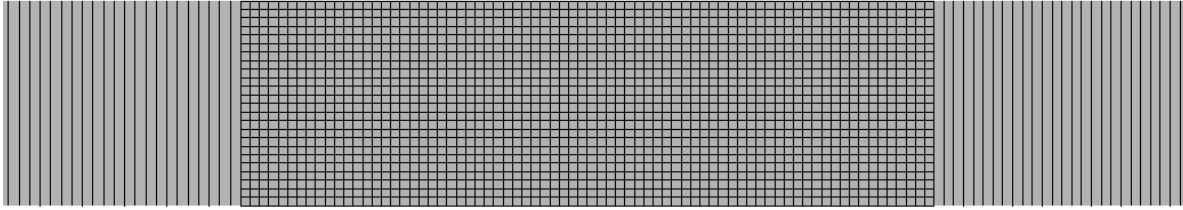


Figure 30. The RTD testing in the shock tube: outside location. The representative pressure profiles recorded by the incident pressure sensor (T4) mounted in the shock tube wall, and three pressure sensors mounted in the RTD prototype and exposed to a single shock wave with nominal intensity of: A) 70 kPa, B) 130 kPa, and C) 180 kPa. The quantification of the peak overpressure values is presented in figure D. Tests were repeated four times at each nominal shock wave intensity.

### Task 6. Numerical Validation of the RTD

Shown above in Figure 17 shows close agreement between the 1D wire model simulation and the experimental shock tube results. Using this initial agreement, an expanded simulation was conducted to evaluate the test specimen area in a 3D environment. The initial driver and driven section take the 1D results and create a curve that is exercised in the 3D test specimen area and the pressure curve measured at the T4 location again. This approach reduces the simulation time while still using the close agreement derived from the 1D wire model. The test specimen area is shown below in Figure 31.



3

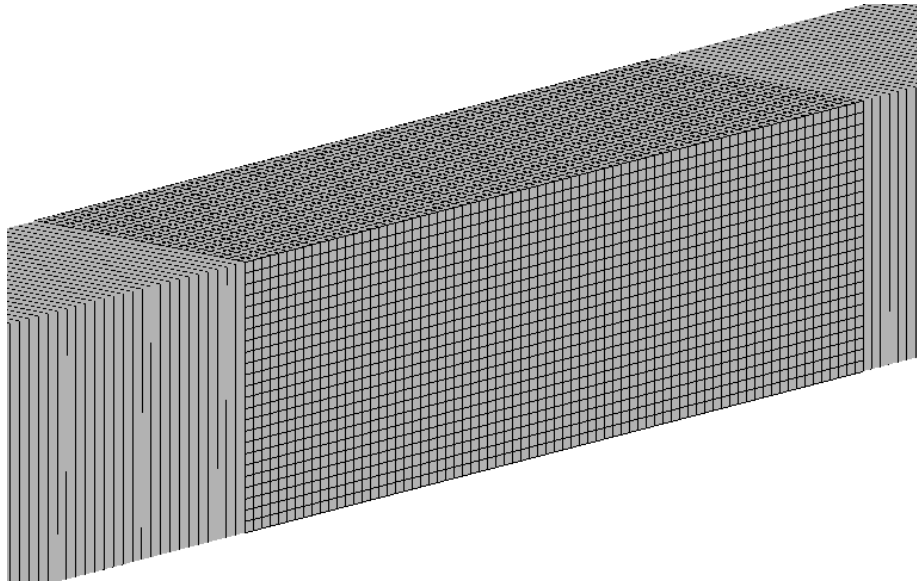


Figure 31. Test specimen area in 3D simulation environment

The results of the 3D simulation are overlaid onto the previously shown data and presented in Figure 32.

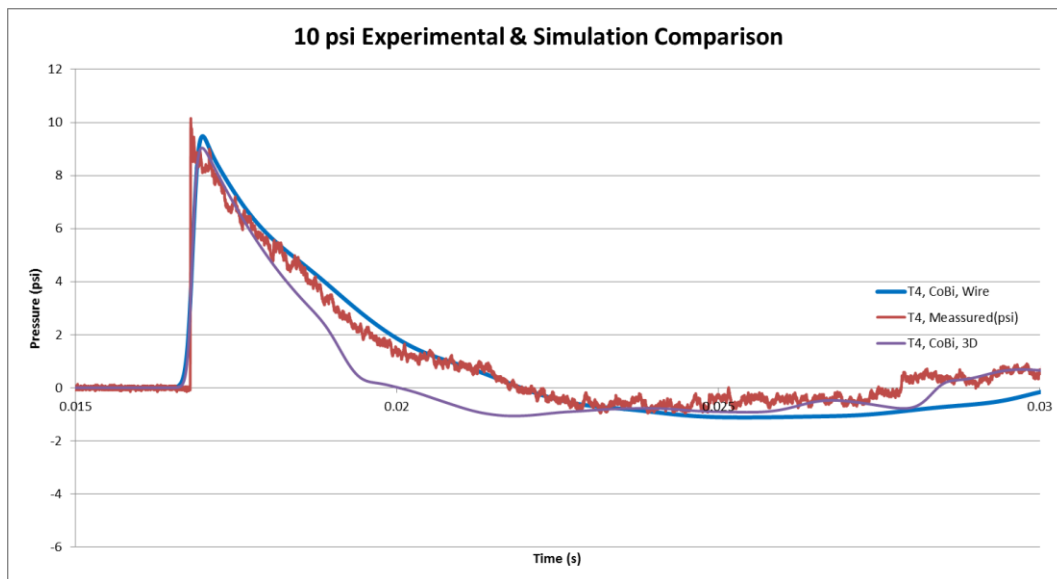


Figure 32. Experimental results compared to 1D and 3D simulation results

As shown in Figure 32, the peak pressure of the 3D simulation has good agreement, but the impulse, or the area under the curve of the primary wave is shorter. This difference was investigated and was likely due to the membrane breakage as the simulations do not fully mimic the breaking of the membrane which is different each time and not easily quantifiable in a simulation. The difference in the experimental and simulation is low (<5%) so confidence remains high that the predicted loads on the RTD are within the expected pressures and loads from the experimental results.

### **3. KEY RESEARCH ACCOMPLISHMENTS:**

The CFDRC/NJIT team is proud of the following key accomplishments:

- First of its kind modular rat test device (RTD)
- Experimentally verified the RTD's operation inside a shock tube under field relevant blast loading conditions
- Virtual shock tube matching experimental shock tube was created and partially validated at the test specimen location

#### **4. CONCLUSION:**

In summary, the CFDRC/NJIT team was able to create a state of the art rat test device (RTD) to measure blast loadings in experimental inside a shock tube meant to mimic field blast conditions in a repeatable manner. A complementary virtual shock tube was also created to allow for predictive investigations of loading scenarios on the RTD to help guide future investigations and experiments. This virtual shock tube also included a virtual RTD which could later be expanded into a higher resolution rat model to look at how those blast loadings effect organs such as the brain, lungs, etc. inside the rat. The desire of the CFDRC/NJIT team is to expand the RTD to include other test article options to create a suite of Blast Test Devices to assist in future blast investigations to the community at large. There remains no good way to correlate individual blast studies and investigations as each study uses different set-ups and devices with no common link. A suite of blast test devices could go a long way in linking these studies together. At the time of writing this final report, the CFDRC/NJIT was informed that the follow on Phase II proposal for this effort was declined. We fully believe this is an important contribution to the DoD, TBI and blast community, as well as larger head/brain damage communities and will pursue other avenues to continue the development of this program.

**5. PUBLICATIONS, ABSTRACTS, AND PRESENTATIONS:**

Nothing to report.

**6. INVENTIONS, PATENTS AND LICENSES:**

Nothing to report.

## 7. REPORTABLE OUTCOMES:

In this six month Phase I program, the CFDRC/NJIT team developed a first of its kind **modular rat test device (RTD)** that has been **experimentally verified** in a shock tube under **field relevant blast conditions** coupled with a partially validated **3-D virtual shock tube**.

**8. OTHER ACHIEVEMENTS:**

Nothing to report.

## **9. REFERENCES:**

Gupta, R.K., and Przekwas, A. (2013) Mathematical models of blast-induced TBI: current status, challenges, and prospects. *Front. Neurol.*, 30 May 2013 | doi: 10.3389/fneur.2013.00059

**10. APPENDICES:**

Nothing to report.